Article

Capabilities of an Acoustic Camera to Inform Fish Collision Risk with Current Energy Converter Turbines

Garrett J. Staines [1,*], **Robert P. Mueller** [1], **Andrew C. Seitz** [2], **Mark D. Evans** [2], **Patrick W. O'Byrne** [3] **and Martin Wosnik** [3]

1   Pacific Northwest National Laboratory, Marine and Coastal Research Laboratory, Sequim, WA 98382, USA; robert.mueller@pnnl.gov
2   Department of Fisheries, College of Fisheries and Ocean Sciences, University of Alaska Fairbanks, Fairbanks, AK 99775, USA; acseitz@alaska.edu (A.C.S.); mdevans@alaska.edu (M.D.E.)
3   Atlantic Marine Energy Center, University of New Hampshire, Durham, NH 03824, USA; patrick.obyrne@unh.edu (P.W.O.); martin.wosnik@unh.edu (M.W.)
*   Correspondence: garrett.staines@pnnl.gov

Abstract: A diversified energy portfolio may include marine energy in the form of current energy converters (CECs) such as tidal or in-river turbines. New technology development in the research stage typically requires monitoring for environmental effects. A significant environmental effect of concern for CECs is the risk of moving parts (e.g., turbine blades) colliding with animals such as fishes. CECs are installed in energetic locations in which it is difficult to operate sensors to fulfill monitoring requirements for informing collision risk. Collecting data (i.e., about blade strikes or near-misses) that inform interactions of fishes with CECs is usually attempted using active acoustic sensors or video cameras (VCs). Limitations of low-light conditions or water turbidity that preclude effective use of VCs are overcome by using high-resolution multibeam echosounders (or acoustic cameras (ACs)). We used an AC at two sites to test its ability to detect artificial and real fish targets and determine if strike, near-miss, and near-field behavior could be observed. Interactions with fish and artificial targets with turbines have been documented but strike confirmation with an AC is novel. The first site was in a tidal estuary with a 25 kW turbine and water clarity sufficient to allow VC data to be collected concurrently with AC data showing turbine blade strike on tethered artificial fish targets. The second site was a turbid, debris-laden river with a 5 kW turbine where only AC data were collected due to high water turbidity. Data collection at the second site coincided with downstream Pacific salmon (*Oncorhynchus* spp.) smolt migration. Physical fish capture downstream of the turbine was performed with an incline plane trap (IPT) to provide context for the AC observations, by comparing fish catches. Discrimination between debris and fishes in the AC data was not possible, because active movement of fishes was not discernable. Nineteen fishes were released upstream of the turbine to provide known times of possible fish/turbine interactions, but detection was difficult to confirm in the AC data. ACs have been used extensively in past studies to count large migratory fish such as Pacific salmon, but their application for small fish targets has been limited. The results from these two field campaigns demonstrate the ability of ACs to detect targets in turbid water and observe blade strikes, as well as their limitations such as the difficulty of distinguishing small fishes from debris in a high-energy turbid river. Recommendations are presented for future applications associated with CEC device testing.

Keywords: marine energy; collision risk; fish; acoustic camera; imaging sonar; current energy converter; turbine; ARIS

1. Introduction

Globally, governments are supporting marine energy as an alternative to carbon-based energy sources such as fossil fuels [1]. Current energy converters (CECs), such as

turbines, are a promising form of marine energy that have recently been tested in rivers and tidal channels where current velocities are sufficient for power generation (e.g., Federal Energy Regulatory Commission Docket P-13511) [2,3]. All technology testing is subject to environmental effects oversight from regulators originating from several authorities (e.g., the Endangered Species Act of 1973), and the risk of collision between animals such as marine mammals, fishes, and diving birds with moving parts, such as turbine blades, is a concern. To address collision risk concerns, monitoring is often required for permission processes such as licensing and permitting [4,5]. To date, assessing the risk of collision has been an expensive and time-intensive requirement that has slowed, and in some cases prevented, the installation and testing of CEC technologies [6,7].

Site locations for CEC installations are in high-energy environments featuring fast currents and often turbid water with low visibility that create a challenging monitoring environment. Previous studies for observing strike, near-miss, and close-range evasion behavior of fishes in the near field of a CEC used video cameras (VCs) and active acoustic sensors such as acoustic cameras (ACs), but there are limitations to each of these technologies. VCs are an effective sensor for monitoring collision risk, and the "movie" data product is recognizable to most regulators and stakeholders, and intuitive to comprehend. However, VCs can only be used when the water is sufficiently clear, and when there is sufficient light (natural or artificial). For example, VCs were used in [8] to monitor for fish strike and near-field behavior around a vertical axis turbine installed in a marine lagoon outlet. Water clarity was sufficient and use of a stereo camera setup allowed for detailed observations of fish behavior around the device, and no strike events were detected. The authors of [9] used VCs to observe fish behavior near an operational commercial-scale turbine and found that as current velocity increased, fish abundance decreased. Artificial lighting was used to facilitate nighttime observations, and strike was not observed in any reviewed data. Artificial lighting was also used to illuminate the field of view of VCs used by [10] where adult and juvenile Pacific salmon (*Oncorhynchus* spp.) were observed near an in-river horizontal axis turbine. The use of artificial lights was critical, because most fish movements occurred at night (possible behavior effects from lights were not addressed). A study in the Kvichak River, in Alaska, showed that under optimal lighting and turbidity conditions, VCs were effective at imaging fish/turbine interactions at ranges up to 4.5 m [11].

Where the usefulness of VCs is limited, ACs provide an alternative observation method. For instance, [12] used a pair of ACs to observe up- and downstream fish interactions with a horizontal axis, crossflow turbine operated from a moored barge. Sampling occurred for ~23 h and VCs would have required lights for nighttime when most fish were observed. No strike events were observed, and various behaviors were defined and quantified. High water turbidity precluded the use of VCs in the East River, in New York, where [13] used an AC from a bottom-mounted platform to observe for collision risk for an axial flow turbine installation in 2012. A multi-sensor platform deployed by [14] for monitoring animal interactions with a potential CEC turbine included a multibeam echosounder (MBES (MBES sensors typically have lower operating frequencies, longer detection ranges, and lower image resolution than ACs)). MBES data informed depth preferences for animals including fishes, general interaction observations, and the development of algorithms for automatic target detection and tracking. These multi-sensor platform studies do not propose to provide information about direct animal collisions such as blade strikes because they are difficult phenomena to observe with MBES, but to provide data needed for modeling encounter rates and collision risk based on depth and animal behavior. While there are many advantages to using ACs for collision risk monitoring, such as their ability to "see" in turbid water, there also are limitations to their applications.

ACs have several limitations relative to VCs. ACs lack the resolution of VCs, which reduces the number of pixels that make up an image. The size of each pixel for ACs is also variable as a function of range and individual beam width [15]. These characteristics affect target detection and classification capabilities, especially for small targets at long ranges

relative to the operational frequency of the AC. Movement is often used to classify targets and this is difficult to detect when the targets of interest are small and consist of only a few pixels in a sequence of images. Image production is slower for ACs than for VCs, which limits the maximum attainable frame rate. Reduced frame rate limits movement observation as a means of classification when fast-moving targets are detected with slow frame rates. The combination of image production time, slow frame rate, and fast-moving targets can even lead to parts of targets missing from images. VCs are challenged by particles in the water column that scatter light, thereby reducing the contrast of targets in images. Similar challenges exist for ACs because particles such as small organic debris and entrained air scatter sound, attenuating transmission and signal reception that increase background noise (volume scattering) and resulting in reduced signal-to-noise ratios. Knowledge of AC limitations is important for effective planning and application to inform determinations of collision risk.

The goal of this paper is to describe the efficacy of using ACs to capture information about fish interactions around operational CEC turbines in two different environments—a tidal estuary with relatively non-turbid water and a highly turbid riverine environment. To accomplish this goal, we had two objectives: (1) to inform blade strike detection by comparing concurrent AC and VC data collection results; and (2) to observe fish near an operational turbine using an AC in a turbid river and document their interactions and behaviors. Collected data highlight the strengths of ACs as well as limitations of their use and helped inform recommendations for future use of ACs at current energy sites and areas of future research. The findings presented in this paper will help researchers choose when to use ACs and how best to apply them, considering their orientations, operating frequencies, and data collection parameters. Maximizing the productive use of ACs along with other sensors to inform determinations of collision risk will provide regulators with needed empirical field campaign results to inform their decision making. This in turn will facilitate more efficient regulatory processes for CECs.

2. Materials and Methods

Data are presented from two test sites. The first is the University of New Hampshire Tidal Energy Test Site at Memorial Bridge (Test Site 1), which was accessed on 13 May 2021. The second is the University of Alaska Fairbanks (UAF), Tanana River Test Site (Test Site 2), which was accessed in the period of 14–17 June 2021.

2.1. Test Site 1

Test Site 1 (Figure 1) is located at Memorial Bridge in Portsmouth, NH, in the Great Bay Estuary (GBE). The GBE system is an energetic, tidally driven estuary on the East Coast of the United States that connects the Gulf of Maine to Great Bay, NH. The GBE is a tidally dominated, well-mixed system with near ocean salinity [16,17]. The site has a nominal depth of 18 m, a maximum tidal range of approximately 4 m, and tidal currents can exceed 2.5 m·s^{-1} during spring ebb tides. On the Portsmouth-facing side of Pier 2 of Memorial Bridge, a Turbine Deployment Platform (TDP) is operated outside the shipping channel.

The TDP (Figure 2) is nominally 15 m in length and 6 m in width and is moored to the pier cap via vertical guideposts 7 m in height, allowing vertical movement with changing water levels. High-density polyethylene pontoons were used for buoyancy and a galvanized steel frame for structural strength. There was an opening ("moon pool") in the middle of the platform that is 5.7 m in length and 3.4 m in width, through which a New Energy Corporation (Calgary, AB, Canada) EnviroGen, series EVG-025H, 25 kW-rated turbine was deployed. The turbine was a four-bladed, vertical axis, crossflow design and was 3.2 m in diameter and 1.7 m in height. More information about the test site can be found in [18–20].
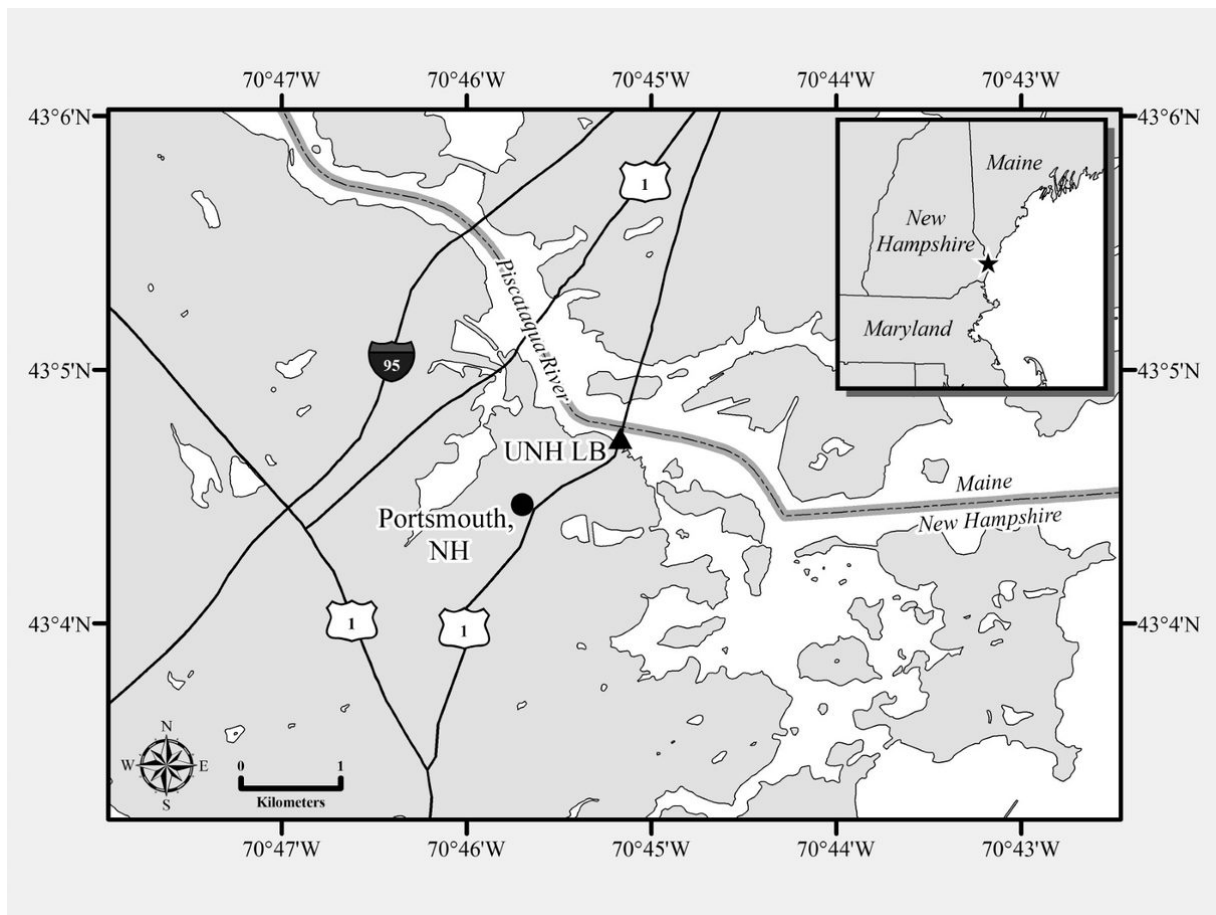
Figure 1. Location of the University of New Hampshire Tidal Energy Test Site at Memorial Bridge on the Piscataqua River in New Hampshire, USA.

Current velocity data were collected using a LinkQuest Inc. (San Diego, CA, USA) FlowQuest 1000 acoustic Doppler current profiler operating at 1000 kHz and installed from a pole mount upstream of the turbine during flood tide (Figure 2), indicating that currents ranged from 0.51 to 0.90 m·s^{-1}. Turbine rotations per minute (RPM) ranged from 10.5 to 14.0 RPM.

A Sound Metrics Corporation (SMC) (Bellevue, WA, USA) Adaptive Resolution Imaging Sonar (ARIS) 3000 Explorer was used to observe the rotating turbine and water flowing into it during a flood tide. The ARIS was mounted on one end of an aluminum pole 3 m in length. The pole was rigidly mounted on the south side of the TDP (Figure 2), which enabled manual depth adjustments. The ARIS field of view (FOV) was 28° vertical (a spreader lens from SMC was installed to increase the FOV from the standard 14°) and 30° horizontal. The mount included a tilt mechanism allowing the device to be angled vertically up +15° and down −30° from horizontal. For this application, the ARIS was 1.25 m deep and tilted down −0.6°. This provided a FOV during flood tide in which the rotating turbine blades were in the left half (downstream) of the FOV, allowing observation of objects transported by the tidal currents coming from the right half (upstream).

The ARIS can operate at two frequencies, 1.8 MHz and 3.0 MHz, with the lower frequency providing longer detection ranges. The FOV is made up of an array of individual beams that are 0.3° by 14°, and each beam is separated by 0.25°. Data can be collected with 128 beams that duty cycle through eight pings or using 64 beams that duty cycle with four pings as a tradeoff for faster frame rates at the expense of decreased horizontal resolution. The maximum achievable frame rate is 15 frames per second (fps). Data collection was conducted at 1.8 MHz operation frequency, maximum transmit power, the "Wide" setting

for pulse width, and default gain of 12 decibels. Data were collected at 15 fps, with a sample range start of 0.7 m, a sample range end of 4.1 m, and a beam focus range of 2.73 m. The ping mode setting was 128 beams/8 pings. For this application of the ARIS, the nominal cross-range resolution was 3 mm at 0.7 m (start of sampling range) to 16 mm at 4.1 m (end of sampling range). The down-range resolution was constant at 3 mm. Basic principles and operating procedures of the ARIS (and SMC technology) AC can be found in [15].
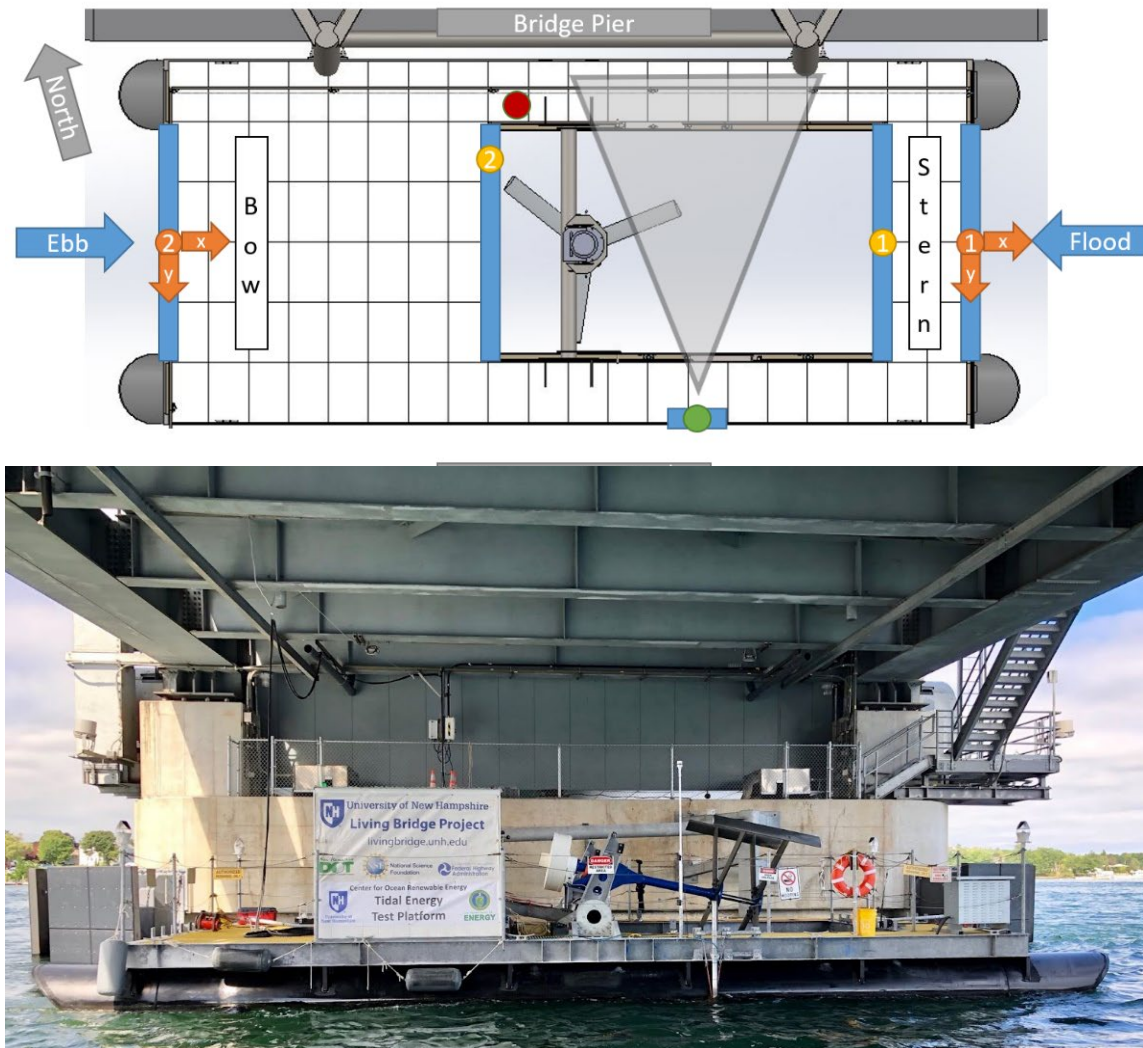

Figure 2. Top: Plan view of the University of New Hampshire Tidal Energy Test Site at Memorial Bridge Turbine Deployment Platform (TDP) showing the field of view (gray triangle) of the acoustic camera and installation location at the green circle. Orange circles "1" and "2" are the acoustic Doppler current profiler locations. The yellow "1" is the location of the video camera and artificial targets deployment. **Bottom**: Photograph of the TDP with the turbine in a raised position located on the Portsmouth, NH-facing side of Memorial Bridge Pier 2.

Concurrent VC data were collected using a GoPro, Inc. waterproof HERO7 at 30 fps, 1920 × 1080 pixel resolution, using the image stabilization function and a flat lens. The camera was attached to one end of a pole 2.5 m in length. Four fishing lures (artificial targets) were deployed underwater upstream of the operational turbine to observe blade strike with the ARIS and the GoPro (Table 1). Each artificial target was attached to 1.8 m of monofilament nylon fishing line and the other end of the monofilament was attached to the wooden pole in the same location as the GoPro. The artificial target was lowered into the water upstream of the turbine allowing the current to pull it taut, followed by lowering the

camera into the water. This allowed the camera to capture the underwater movement of the artificial target upstream of the rotating turbine blades. The water current maintained tension on the monofilament and the artificial target was allowed to slowly move back toward the rotating turbine blades until strike occurred. This action was repeated with all four artificial targets, while capturing concurrent ARIS data. Artificial targets two and three were unintentionally allowed to drift past the path of a turbine blade resulting in the blade striking the monofilament and severing the connection.

Table 1. Artificial targets with size, material, and turbine details used in video camera and acoustic camera observations at the University of New Hampshire Tidal Energy Test Site at Memorial Bridge.

Target	Length (cm)	Material	Current Velocity ($m \cdot s^{-1}$)	Turbine [1] RPMs	Supplementary Video
1	8.0	Hard plastic	0.85	13.4	Video S1
2	10.0	Hard plastic	0.90	11.9	Video S2
3	10.0	Hard plastic	0.71	14.0	Video S3
4	10.5	Soft rubber	0.80	11.8	Video S4

[1] Rotations per minute.

ARIS and GoPro data were visually processed by viewing each data file concurrently. This allowed for a head-on (downstream) GoPro perspective of the artificial fish targets attached to monofilament, while the ARIS provided a perspective of "looking down" or a plan view. The GoPro view allowed the viewer to determine if the artificial fish target was struck by the turbine blade in each file. Then, the strike instance was confirmed by viewing the ARIS file for instances of each of the four artificial fish target strikes. Blade strike was determined to have occurred when a sudden change in its movement was observed in conjunction with a significant lateral shift in location.

2.2. Test Site 2

Test Site 2 is the Tanana River Test Site (Figure 3), a fully permitted location on the Tanana River near Nenana, AK, that is operated by the UAF as a part of the Pacific Marine Energy Center. At Test Site 2, the Tanana River is approximately 150 m in width and has a nominal depth of 6–8 m [21]. The current velocity typically flows 1–2 $m \cdot s^{-1}$ but can vary from 0.5 $m \cdot s^{-1}$ in winter months to 2.5 $m \cdot s^{-1}$ during summer months, and over 3.0 $m \cdot s^{-1}$ during high-water events [22]. Average river discharge during the sampling period came from the U.S. Geological Survey Tanana River gauging station (64°33′53.8′ N, 149°05′38.4′ W), located ~2 river km downstream of the sampling site. The water is highly turbid as a result of sediment from glacial runoff in the headwaters [23], and surface and suspended woody debris present during the sampling period consisted of small (fibrous woody debris smaller than 1 cm), medium (items greater than 1 cm such as twigs and sticks), and large (tree trunks and root wads) items [22]. Much of the debris was diverted around the research platform surface expressions by the research debris and diversion platform (RDDP), which was designed to divert debris around turbines and can support impact forces of up to 22,680 lb [24]. Typically, peak Pacific salmon smolt out-migration in the Tanana River occurs in May and June [25] and the timing of the field campaign at Test Site 2 was aimed to avoid early-season runoff and debris loads, thereby reducing risk to equipment and sensors, but still enabling the capture and observation of downstream migrating Pacific salmon smolts (chum *Oncorhynchus keta*, Chinook *O. tshawytscha*, and coho *O. kisutch* salmon).

The turbine operations and data collection occurred on four connected, moored research platform surface expressions in the main channel of the river (Figure 4; from upstream to downstream): the RDDP, a research barge for instrumentation deployment and data collection, the TDP, and an incline plane trap (IPT).
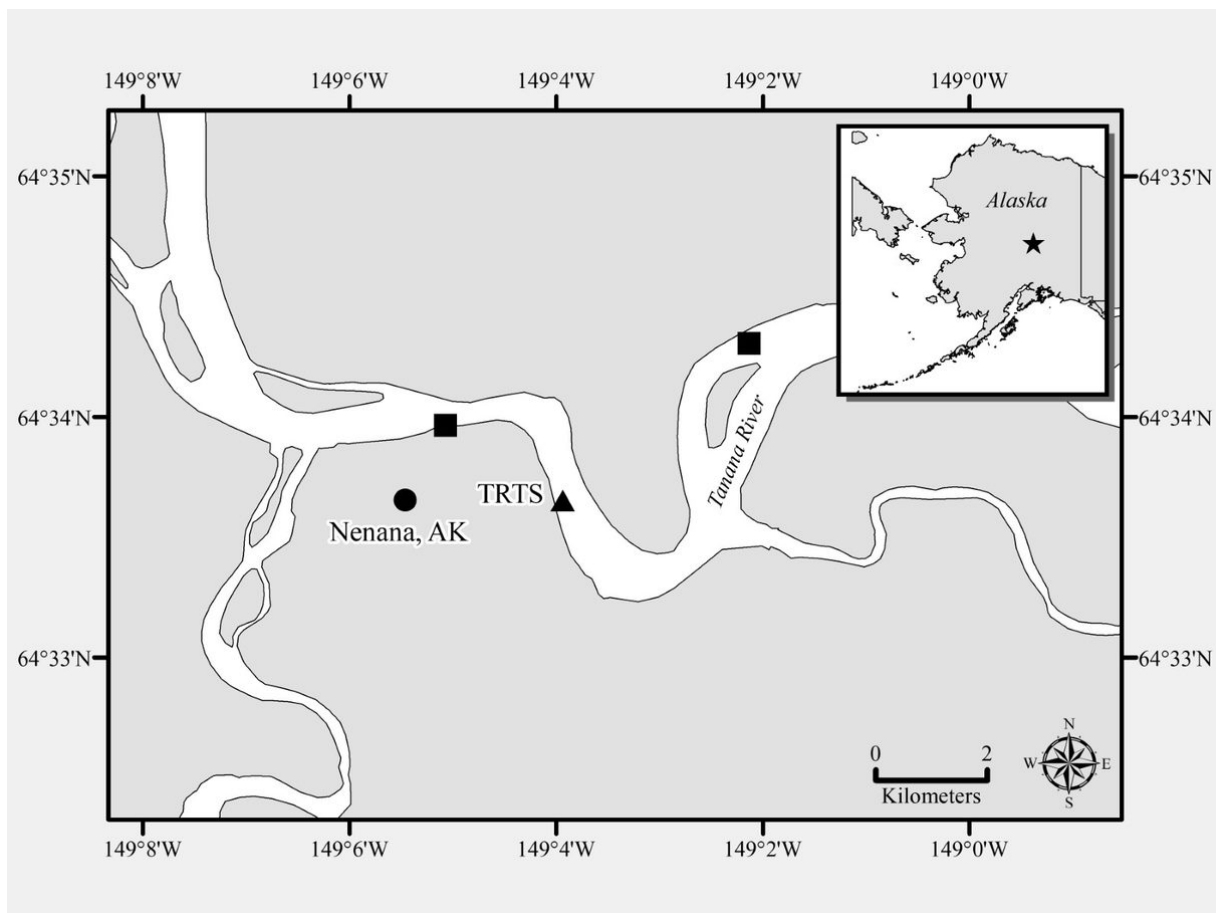
Figure 3. Test Site 2 location at the Tanana River Test Site (triangle) near the city of Nenana, AK, USA. General locations for fyke net sets are indicated with squares.

The research barge is an aluminum platform attached to two aluminum pontoons and is nominally 12.2 m in length by 6.1 m in width and has an opening ("moonpool") that is 3.6 m in length by 3 m in width. This was the main platform for sensor attachment and transfer of personnel and equipment to and from shore. The turbine barge consists of two aluminum pontoons with an open region in which the turbine can be manually pitched and lowered. A 5 kW New Energy EnCurrent (Calgary, AB, Canada) vertical axis turbine model EVG 005H was deployed and used for the AC evaluation. The turbine had a main shaft length of 2.3 m with four vertical blades (1.4 m in length and 15.2 cm in width) that featured a swept diameter of 1.5 m. The IPT sampled fishes in the top 1.1 m of the water column downstream of the turbine (Figure 4). Current velocity data were collected using a Teledyne (Thousand Oaks, CA, USA) RiverPro ADCP operating at 1200 kHz installed on the front of the research barge (Figure 4). Turbine RPMs were not available at Test Site 2.

Test Site 2 is known to have out-migrating Pacific salmon smolts during our sampling time frame [21,26], and ARIS data were collected to observe fishes moving downstream that may pass near, into, or around the turbine. ARIS data were collected in 10 min files and with the same pole and tilt mount used for Test Site 1. The pole mount location was on the port side stern of the research barge (Figure 5) with the ARIS aimed 15° downstream from orthogonal to the current to capture the rotating turbine blades on the right side of the FOV (downstream) and objects flowing into the turbine from left (upstream) (Figure 5). Tilt angles varied by day. The same ARIS data collection settings were used at Test Site 2 as at Test Site 1 except that the start range was 1.7 m, the end range was 5.9 m, and focus range was 3.7 m. Four days of data collection occurred with a total of 15.25 h of data when the turbine was deployed (rotating and stationary). Each

day had different orientations (Table 2) of the ARIS to provide information about the best aiming location for this project and to provide recommendations for future applications of using ACs for informing determinations of the risk of fish collision with CECs. Turbidity in NTUs was measured each morning using a Hach (Loveland, CO, USA) model 2100P portable turbidimeter.
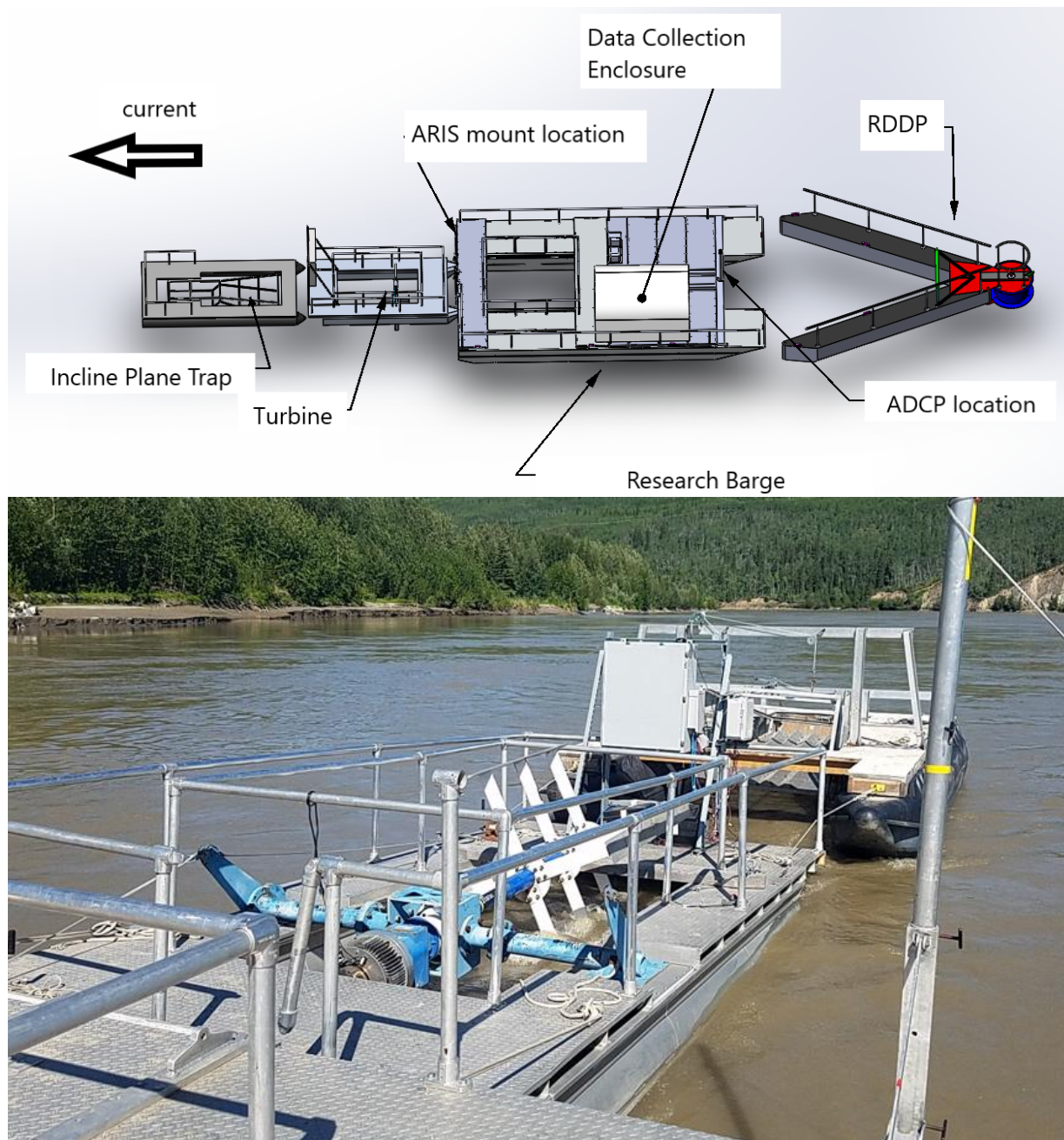

Figure 4. (**Top**): Schematic of connected surface expressions at the Tanana River Test Site, illustrating the main components of the system: research debris and diversion platform, research barge, turbine barge, and incline plane trap. (**Bottom**): Turbine barge with 5 kW New Energy EnCurrent turbine in a raised position. The IPT is attached to the stern of turbine barge, which is attached to the stern of research barge.
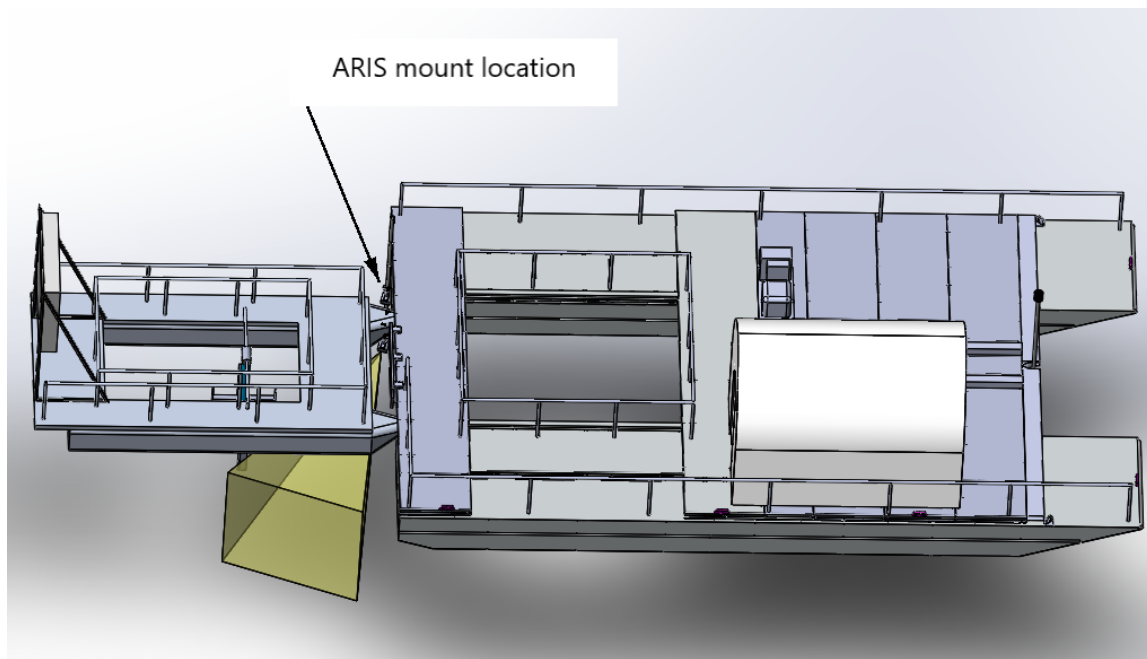
Figure 5. ARIS sonar beam sampling field of view in relation to the turbine at the Tanana River Test Site near Nenana, AK. The current direction is from right to left.

Table 2. ARIS orientation for each day of data collection along with amount of data accumulated by the time when the turbine was deployed (operating and static) and turbidity measure each morning at the Tanana River Test Site, near Nenana, AK.

Day	Tilt (deg)	Depth (m)	Turbidity NTUs [1]	Mean Current Velocity (m·s^{-1})	Average Discharge (m^3·s^{-1})	Data Volume (h, GB)
14 June	0.0	0.75	211	n/d	1113	3.1, 22
15 June	−0.4	2.4	209	1.67	1138	4.8, 34
16 June	−9.7	1.0	227	1.64	1175	3.9, 28
17 June	−9.4	1.0	263	1.71	1223	3.5, 25

[1] Nephelometric turbidity units.

2.2.1. Data Processing

Each 10 min data file was manually processed by a human reviewer using SMC (Bellevue, WA, USA) ARISfish software version 2.6 (ARISfish). Initial screening for targets passing through the FOV was performed using the ARISfish echogram, which is a visual representation of the ARIS data, compressed to a vertical line of pixels for each image frame so the maximum sonar return for all beams is displayed for each range sample. The angular FOV (i.e., all sonar beams) is processed to form each frame line, so fishes swimming within the image can be observed in the echogram. The y-axis contains all sonar returns in the sampled range and the x-axis represents time (i.e., frame number). Targets passing through the FOV create tracks that contrast with the background and can be marked with a computer mouse. After targets were marked in the echogram, they were reviewed in the ARISfish sonar image view, which was used during data collection and is analogous to a VC (sequential frames), to observe target motion characteristics. A target's track through the water is resolvable in range and cross-range dimensions in the echogram, but its shape and movement (e.g., tailbeat) were not distinguishable. The reviewer looked for nonpassive movements (e.g., movement in a direction other than current flow or tailbeat) of the target frame by frame to attempt to categorize it as a fish or debris. The shape of the target was also used during review to remove targets that were confirmed to be debris.

The most efficient approach to reviewing the data in the ARISfish software is in the echogram because doing so allows the viewer to view hundreds of pings of data at once for efficient review. However, the beams that make up the part of the FOV ensonifying the turbine blades creates constant backscatter that varies in range and intensity, making it difficult to visually detect target tracks in the echogram. To reduce the risk that targets were missed due to blade backscatter, a second round of review was conducted using the sonar image view to detect targets moving through the range of the FOV that contained the turbine. The human reviewer paused the file when a target was detected and marked it using the computer mouse. All target markings, whether in the echogram or the sonar image view, were registered in both views. Next, the reviewer scrolled through each data file using the sonar image view to find the frame that provided the best image of each target and used the ARISfish software measurement function to measure its length. ARISfish has a function to sequentially move through each marked fish without scrolling through empty time blocks of a full data file, which reduced the overall processing time. The computer mouse was used to click the beginning and end of each target, resulting in a measurement registered along with a range annotation that were stored for later analysis. ARISfish software creates comma-separated values files for each processed data file that includes the range of all marked targets and the manually measured length.

A subsample of 12 processed data files from June 17 were timed to the nearest minute for the manual marking of targets. Additionally, one data file was timed for the duration it took to process the measurement annotation for each target. These results are consulted to determine the amount of effort that can be expected for processing ARIS data manually with no automation.

The FOV of an AC expands vertically with range and affects the probability of detecting passing targets. As a result, targets passing near the ARIS were less likely to be detected than those passing farther out. To address this, the number of detected targets were range-normalized by using the following equation:

$$Z = V_{max}/(2 * R_{tar} * \tan (\Theta/2)), \tag{1}$$

where Z is the range-normalized ARIS target value; V_{max} is the maximum vertical dimension of the FOV at the maximum range sampled (5.9 m), which here is 2.94 m; R_{tar} is the range of the target from the ARIS; and Θ is the angle of the vertical dimension of the ARIS FOV, which here is 28°. So, a target detected at a maximum ARIS sampling range of 5.9 m is range-normalized to 1 and values increase for targets as they decrease in range from the ARIS. All targets were then categorized according to the range at which they were detected from the ARIS relative to the range of the turbine. Three range categories were designated. The first range category was "0", which was 1.7–2.0 m (0–1.7 m was not sampled) from the ARIS and represented the range in which targets would pass between the ARIS and the near edge of the turbine. The second range category was "1", which was 2.0–3.5 m and represented the range in which targets would pass between the near and far edge of the turbine. These targets could possibly go into the turbine and possibly be sampled by the IPT. The third category was "2", which was 3.5–5.9 m and represented the range in which targets would pass beyond the far edge of the turbine and the end of the sampled range window (Figure 6).

A cross-sectional area was calculated for range category "1" to provide a sampled area in front of the turbine and for comparison to the IPT fish catches downstream. Range category "1" consists of water upstream of the turbine and the IPT, which sampled water that flows into the turbine and is partially sampled in the top 1.1 m of the water column by the IPT (Figure 6). An analog to catch per unit effort (CPUE) was calculated for non-range-normalized ARIS targets (referred to as ARIS CPUE) for range category "1" by dividing the number of targets detected by the time duration of sampling per day. Because the cross section sampled by the ARIS and the IPT differ, the number of non-range-normalized ARIS targets for range category "1" was adjusted based on the ratio of cross-sectional areas

sampled by each method (i.e., the sampled cross-sectional area of range category "1" was divided by the sampled cross-sectional area of the IPT).
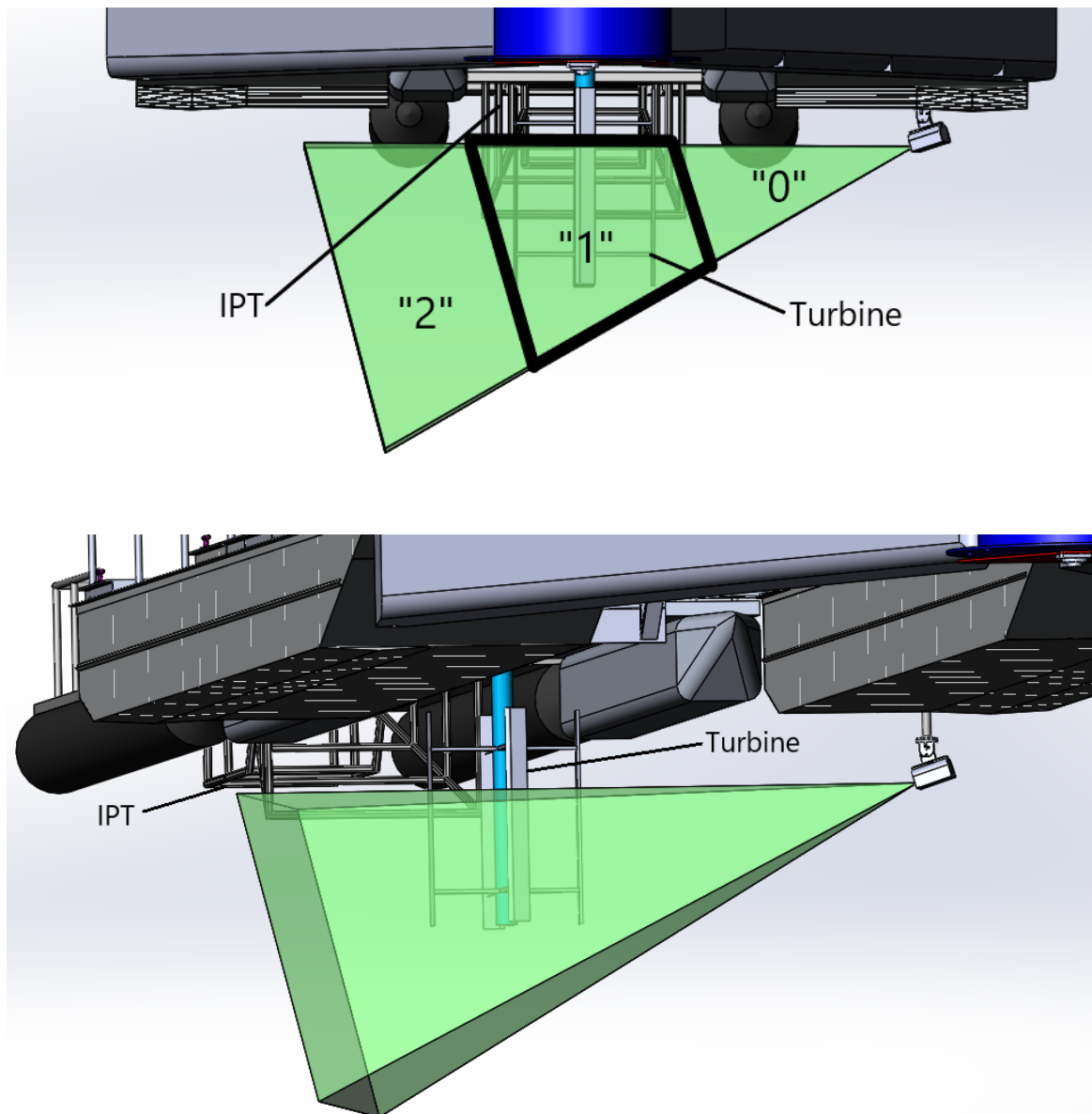

Figure 6. (**Top**): Downstream view as water flows into the page through the ARIS field of view (green triangle), through the turbine, and into the incline plane trap (IPT). The ARIS FOV is labeled according to the range categories in which data were processed. Range category "2" is 3.5–5.9 m, "1" is 2.0–3.5 m, and "0" is 1.7–2.0 m from the ARIS. The start range for the beginning of sampling was 1.7 m and ranges less than that were not included in the data collection. (**Bottom**): Downstream view at approximately 30° rotation from the port (left) side of the surface expressions to provide clear perspective of sequence of ARIS FOV, turbine, and IPT.

2.2.2. Physical Fish Capture

Fish sampling immediately downstream of the turbine was accomplished using the IPT that was attached via line and cleats to the turbine barge (Figure 4). The IPT had two primary sections: the trap followed by the live box. The trap portion was composed of an inclined plane supported by a frame and had a front opening that was 1.1 m in height × 1.5 m in width [27]. When the inclined plane was lowered into the current, the top 1.1 m of the water column was sampled. The total sampling time for all four

days was 14.05 h and the average sampling time per event was 1.08 h. The IPT CPUE was calculated daily as the number of fish caught divided by the time the incline plane was submerged.

To augment the number of fishes naturally migrating through the ARIS FOV, that occurred in low densities, fish sampling was conducted in the river margins for non-salmonid species that were translocated and released from the research barge upstream of the ARIS FOV. In the period 14–17 June 2021 (Figure 3), two fyke nets (1.2 m × 1.2 m frames, dual 9.1 m wings, and 1.27 cm mesh) were placed immediately adjacent to the shore. Fyke nets were fished up to 24 h per day but checked at least twice a day. All fish collected in the nets were classified by species. For each fyke net set, only longnose sucker (*Catostomus catostomus*) and lake chub (*Couesius plumbeus*) were measured, held in a bucket, and translocated to the research barge for release upstream of the turbine. These fishes were called proxy fish. During the four days of ARIS data collection, 16 proxy fish (three were recaptured and rereleased for a total of 19) were released 7 m upstream of the turbine to create a time when a fish target of known size and species could potentially interact with the turbine. A human reviewer observed in real time during each release to document if the fish was seen in the ARIS. Subsequent processing of these events was conducted after field data collection that consisted of reviewing each ARIS data frame for a five-second window after the recorded event time. All targets seen in the ARIS were documented.

3. Results

3.1. Test Site 1

Blade strikes were observed with the GoPro and ARIS on all four artificial targets deployed (Supplementary Videos S1–S4). For artificial targets two and three, there were 9 and 11 ARIS frames, respectively, in which the artificial targets can be seen to drift downstream after being severed from the monofilament.

3.2. Test Site 2

There were 4044 range-normalized targets (1572 non-range-normalized) when the turbine was deployed (operation status varied based on river current velocities) from 14 June to 17 June. A total of 1326 of range category "0" targets had average lengths of 87 mm; 2602 of range category "1" targets had average lengths of 77 mm; and 116 of range category "2" targets had average lengths of 91 mm (Figure 7). These length measurements are all larger than the average length of fishes captured in the IPT, which was 68 mm.

The ARIS sampled cross section of range category "1" (i.e., possibly into the turbine and possibly sampled by IPT) was 2.1 m^2 (Figure 6). No targets exhibited nonpassive movement precluding the manual reviewer from confidently classifying them as fishes instead of debris. The ARIS CPUE per day for non-range-normalized targets for range category "1" ranged from 12 to 71 (Figure 8).

The IPT sampled from 15–17 June 2021 for a total of 14.22 h and caught 25 fishes. Immature Pacific salmon (11 chum, 8 Chinook, and 3 coho) made up 77% of the catch, while 1 each of Arctic lamprey (*Lethenteron camtschaticum*), burbot (*Lota lota*), and lake chub made up the remainder. The Chinook salmon, coho salmon, lake chub, and burbot ranged in length from 50 mm to 115 mm. Most chum salmon smolts were not measured in IPT catches because of their fragility, but based on [26] chum salmon smolts captured in the Tanana River main river channel averaged 42 mm and this value was used to calculate the mean length of all fishes captured in the IPT. Using this average and the actual measured lengths of other species captured in the IPT, the average length of fishes for all four days was 68 mm. Daily IPT CPUE ranged from 1.17 to 2.56 (Figure 8). The IPT sampled a cross-section area of 1.65 m^2, which was lower than that for the ARIS for range category "1", which sampled 2.06 m^2.
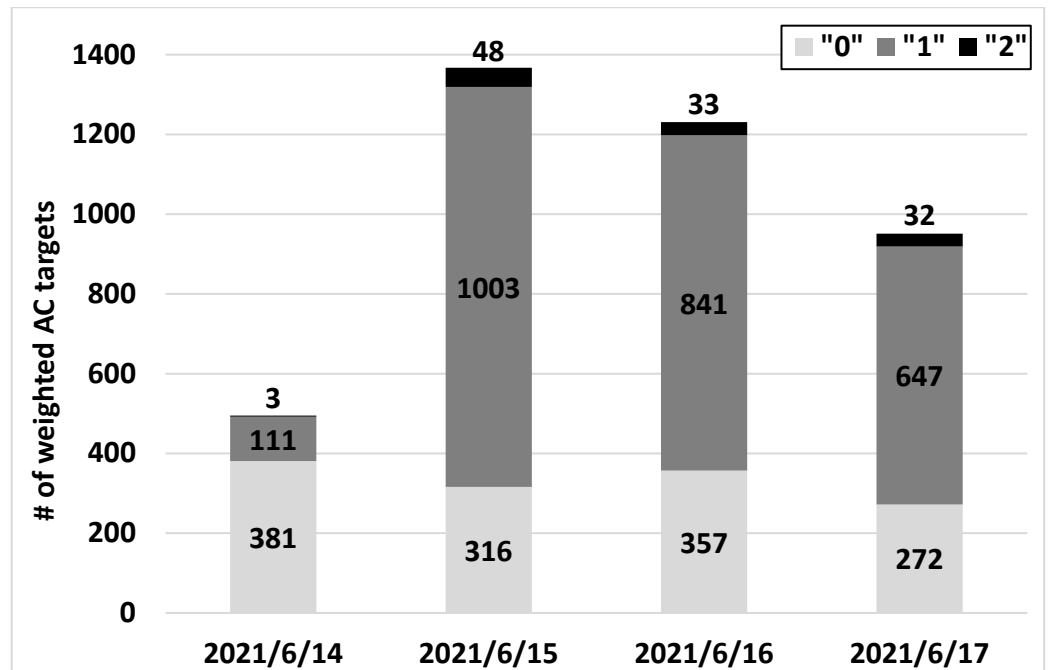
Figure 7. The number of ARIS targets range-normalized for sampling detection by day at the Tanana River Test Site, near Nenana, AK. Each day's sampling is separated into range categories "0", "1", and "2". The average length of targets was 87, 77, and 91 mm for range categories "0", "1", and "2", respectively.
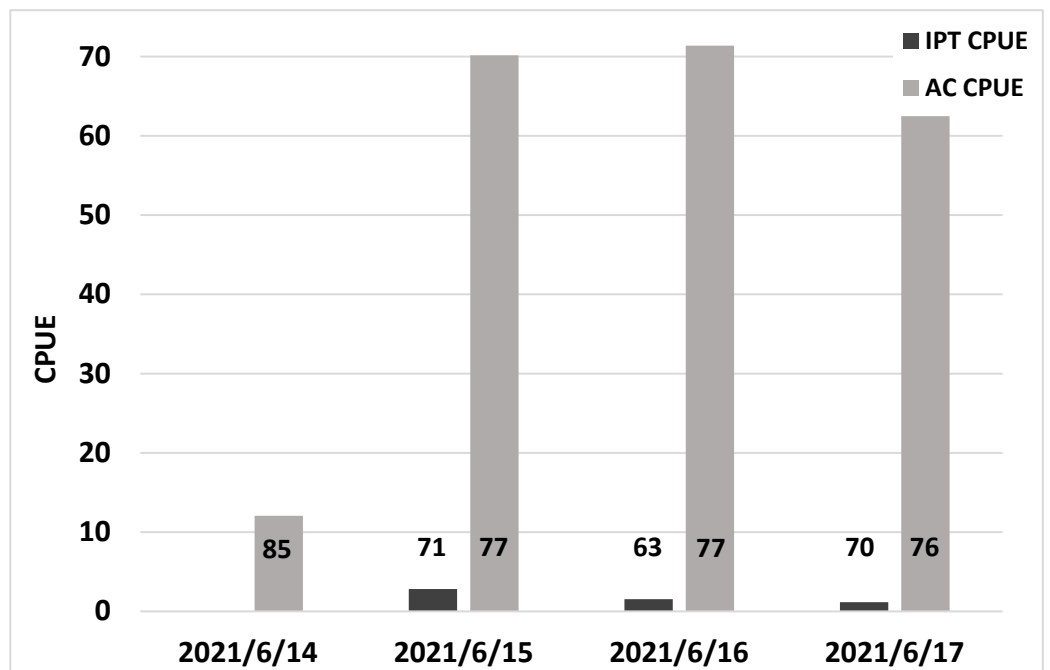

Figure 8. The incline plane trap (IPT) catch per unit effort (IPT CPUE; fish or targets/day) is dark gray and the ARIS CPUE for range category "1" is light gray. The IPT was not fished on June 14. ARIS CPUE was adjusted to account for its sampling more water than the IPT. Values in the bars are average fish length (mm) for IPT and average target length for the ARIS.

Most targets marked during ARIS data processing had gaps in them in images as a result of motion artifacts [28]. The human reviewer saw each target with gaps in them but frame by frame images were consistent and easy to follow and there was no mistaking a

single target with gaps for multiple smaller ones. Figure 9 shows consecutive frames of a target at approximately 2 m from the ARIS where these gaps were observed.
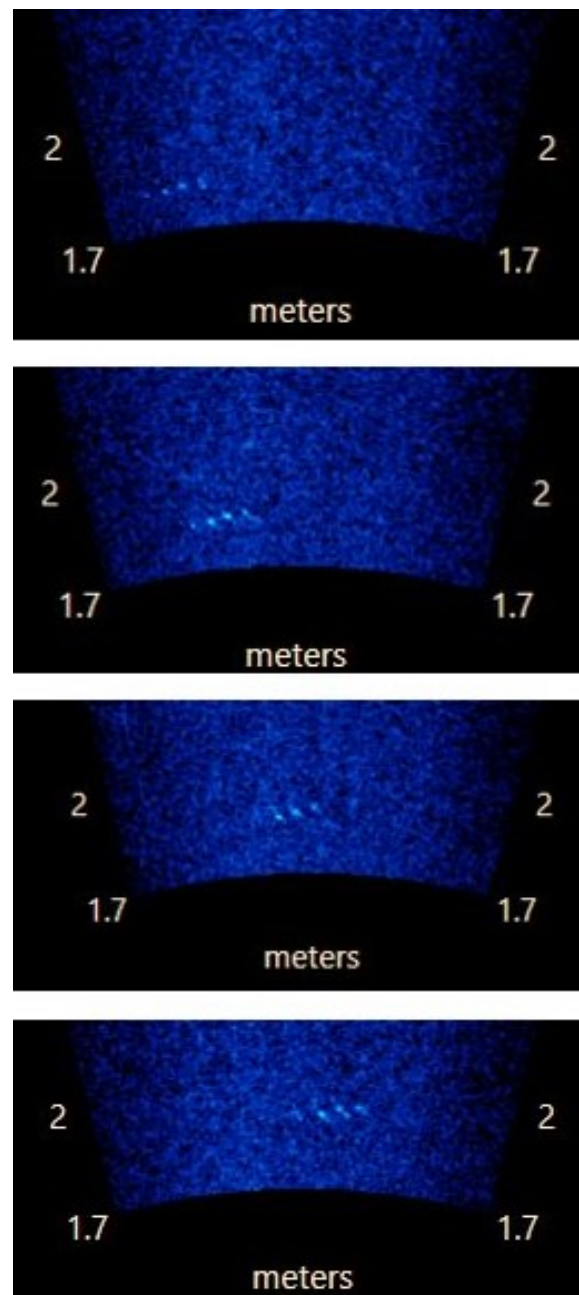

Figure 9. Four temporally successive ARIS frames from top to bottom illustrating the multi-ping acquisition of sequential image frames. The dark blue point-cloud is the ARIS FOV, and the speckle is the constantly present volume backscatter of the water column. The brightest specks in the FOV represent a small target moving through the ARIS field of view (FOV) from left to right (up- to downstream) at a velocity of approximately 1.7 m·s^{-1} at the Tanana River Test Site. The breaks in the target are a result of motion artifacts that occur as a result of the target moving faster than the multi-ping acquisition can assemble the image frames.

Seventeen fyke net sets captured 2360 fishes. Chum salmon smolts made up 97.2% of the catch and whitefishes (*Coregoninae* spp.), longnose sucker, lake chub, and Arctic lamprey made up the remaining 2.8%. Six lake chub and 10 longnose suckers were held for translocation and release upstream of the ARIS in seven events. Three of the 16 fish

released were recaptured in the IPT and rereleased for a total of 19 releases. Of the 19 fishes released, 2 were observed in the ARIS data and 2 were indeterminate, but possible detections (Table 3).

Table 3. Fish sampled from the IPT from fyke net captures. (LNS = longnose sucker; CHB = lake chub.)

Event	Date	Time	Species	Fork Length (mm)	IPT Recapture (Y/N)	Re-Release After Recapture? (Y/N)	Visually Detected (Y/N/M) [1]
1	14 June 2021	15:51:00	LNS	70	N	NA	N
			CHB	120	N	NA	
			LNS	60	N	NA	
2	15 June 2021	13:48:27	LNS	48	N	NA	Y
3	16 June 2021	12:27:18	LNS	40	N	NA	Y; M
			LNS	45	Y	NA	
			LNS	45	Y	NA	
			LNS	45	N	NA	
			CHB	65	N	NA	
			CHB	50	N	NA	
4	16 June 2021	12:40:19	LNS	45	N	Y	N
			LNS	45	N	Y	
5	17 June 2021	11:26:28	LNS	65	Y	NA	N
			LNS	80	N	NA	
			LNS	55	N	NA	
			CHB	100	N	NA	
6	17 June 2021	11:30:22	LNS	65	N	Y	N
7	17 June 2021	16:35:20	CHB	70	N	NA	M
			CHB	70	N	NA	

[1] Y = yes, N = no, and M = maybe.

The average time to process the 12 subsampled data files from June 17 for manual marking of targets was 14 minutes and the average time to measure each target in the first subsampled data file was 15 s.

4. Discussion

4.1. Test Site 1

At Test Site 1, by using tethered artificial targets and review of the underwater video footage showing target and blade interactions, we were able to confirm the capability of ARIS for observing blade strikes of targets. In the ARIS imagery, the tethered artificial fish targets were pushed sideways against the current when struck by a turbine blade, but the tether did not allow the targets to naturally drift downstream as a natural fish would if disoriented or stunned. Instead, the artificial fish target righted itself and returned to a location in the water upstream of the rotating turbine blades and tight against the monofilament tether. There were two instances when the target was severed from the monofilament tether and the target was observed in subsequent ARIS frames as the currents carried it downstream and out of the FOV (Supplementary Videos S2 and S3). These two instances were examples of what a fish strike event might look like when a struck fish is stunned or killed and drifts passively downstream. Improving knowledge about blade strikes is important because, to date, literature has reported difficulty in observing the area just in front of moving turbine blades where a strike or near-miss event would occur [8,13,29]. Similarly, in laboratory flume experiments in which fish were observed entering the test turbine with video and ACs, strikes or near-misses were not visibly determined, and survival and injury rates were used as effect metrics [30,31]. While near-

miss events are important to record and may have impacts on fish, they are likely to have less of an impact on an individual's fitness than strikes. Confirming that the blade strike of a fish could be measured is important for the monitoring campaigns of CEC installations. Empirical results will be crucial for regulators making decisions about present and future monitoring requirements and the associated installation permitting and licensing process.

4.2. Test Site 2

Fish in the Tanana River are of sufficient size to be detected using the ARIS 3000 Explorer AC, but some limitations make this challenging. Pixel size limits the size of detectable targets an AC can detect [32], although the resolution of the ARIS is higher than comparable technologies with more beams and range samples per beam than SMC's previous AC technology, Dual-Frequency Identification Sonar (DIDSON) AC technology [12,33–35]. For example, if the target of interest is larger than the pixel size in the range of interest, then detection is possible. The smallest target expected in this study, a small chum smolt 38 mm [26] in length, will take up two pixels at a range of 5.9 m (pixel size 23 mm in width by 3 mm in length) and five pixels at a 2.0 m range (pixel size 8 mm in width by 3 mm in length). So, all fish are expected to be larger than the biggest pixel and therefore detectable. Furthermore, before collecting data at Test Sites 1 and 2, tests were conducted at Pacific Northwest National Laboratory's Marine and Coastal Research Laboratory in Sequim, Washington, by observing soft-bodied fishing lures in sizes down to 30 mm. These tests were conducted in a freshwater tank out to ranges of 2.5 m and from a research pier in ocean water out to 5 m. Detection of fishing lures was confirmed in all cases. While detection was theoretically confirmed with known pixel resolution of the ARIS data and experimentally confirmed with tank and in situ tests using fishing lures, classification often requires more than the target of interest being larger than sample pixels. The fewer pixels a target is made up of, the fewer features of the target are discernable and the more difficult it will be for a reviewer or computer algorithm to detect motion such as tail beat [36,37]. Fewer pixels per target also create challenges in separating the target of interest from background speckle noise or targets of similar size such as debris. As a result of these combined factors, target detection was achieved at Test Site 2 but classification of fish from debris was not possible.

Another challenge faced when attempting to classify fish from debris was that nonpassive behavior was not observed. Additional information about targets, such as movement and size, are important for classifying them as fishes or debris, which was not possible with these data. Observing the movement of AC targets can be a useful classification method when designating them as fish or debris. For instance, a change in direction or change in acceleration [12,38] can be used to classify a target as being nektonic, especially in the presence of other passively moving targets such as debris. At Test Site 2, there was a lot of debris in the river and migrating Pacific salmon smolts are likely to move with the current [39] for efficient downstream migration. If nonpassive behavior was observed, it could have been used to separate fish from debris, but none of the ARIS targets in this study showed movement independent of the current speed, precluding classification.

Indirect inference can be made about the efficacy of ACs by examining correlations in catch and AC data. Physical fish capture for species and size distributions is commonly used to supplement data from echosounders and other active acoustics sensors when they are used for fish abundance estimates or stock assessments [40]. Here, we looked for similarities to ARIS catch data, ARIS target counts, and ARIS length estimates. The IPT CPUE was much lower than that of the ARIS in range category "1" (Figure 8), and the average length of fishes captured in the IPT was smaller than targets measured in ARIS data. Because of the noncongruence of the average size of targets and their abundance in IPT and ARIS data, it is likely that the targets observed by the ARIS were a mix of fish and debris.

In addition to the high likelihood that the ARIS is observing a mix of fishes and debris, IPT fish size information is likely more accurate than that provided by ARIS because of technical limitations imposed by AC technology. Length comparisons of IPT catch data

and ARIS targets for range category "1" were difficult because the IPT sample size was small. Specifically, smaller fish are difficult to accurately measure because they take up fewer pixels in an image and the measurement resolution of ACs decreases with range due to beam spreading [35]. The ARIS in this research has a cross-range (width of a single beam in the array) resolution of 16 mm at the 4.1 m range. A fish that is detected in three cross-range pixels at this range will measure 48 mm even if the head and tail take up less than the full 16 mm of the first and third pixel. So, it is possible that the measurement tool in the ARISfish will overestimate the length of small targets because the best measurement resolution is the width of a single beam at the range of the target.

Challenges in confirming fish targets in the ARIS observations may also be related to the speed at which they were moving downriver and the limited amount of time they were in the FOV. Classification of detected targets is more likely to be successful the longer they are in the FOV. Further, ARIS images are vulnerable to motion artifacts if objects moving through the FOV are faster than the time it takes for the camera to complete an acoustic scan and mosaic beam returns into an image [15,41]. Motion artifacts [28,42,43] were observed in the ARIS data collected at Test Site 2 when fast-moving targets spent limited time in the FOV (Figure 8) leading to "broken targets." This phenomenon is most pronounced when objects are oblong in shape and move through the FOV at a high speed along the long axis and at an oblique angle to the ARIS beams. The described motion artifacts in ARIS data have implications for both target classification and length measurements. Challenges related to target classification can also increase manual processing time. This study timed processing for a subsample of data files and each 15-min file takes on average 14 min, not including target measurement. Targets that occur in only a few frames and that are broken will likely take longer to measure with confidence, leading to longer processing times overall. In this study, motion artifacts may have limited the detectable swimming motion of a fish. Motion artifacts can create scenarios where a target can even disappear from a single frame as it moves through the FOV [28].

The challenges presented in classifying targets in this study have been experienced in other applications of ACs. The authors of [44] addressed classification of fish and debris using size and backscatter thresholds. For this approach to be effective, size thresholds require the fish and debris to have known length differences and scattering properties. Discrimination based on length thresholds was not attempted in this study, although anecdotal evidence indicates that the lengths of debris and fish in the IPT overlapped. Backscatter thresholds require knowledge of target backscatter characteristics. At the relatively high operating frequencies of most ACs, the majority of backscatter is contributed by the target surface rather than interior features, such as swimbladders [45]. Therefore, if fish and debris are of the same size and general shape, then surface backscatter may be similar, and classification based on backscatter intensity may not be possible. Even with a high-resolution AC at ranges less than 12 m, [46] was able to identify only 9 out of 15 large targets that all measured over 2 m in length, indicating that classification is still difficult with relatively large, slow-moving targets.

Two unmeasured environmental factors could have reduced the quality of ARIS images and target classification by increasing the background reverberation. Suspended debris is prevalent at Test Site 2 and consisted of fine organic matter as documented previously by [24]. The suspended organic matter was apparent when small lines placed in the water for other tasks would accumulate this fine organic debris and take on a "fuzzy" appearance, but it was not quantified. However, the presence of suspended organic matter in the water column during data collection could have attenuated the ARIS transmissions and returns [47], which would increase background reverberation and reduce the signal-to-noise ratio [48]. A second environmental factor that could have affected ARIS image quality was entrained air of small size known as microbubbles. Microbubbles reduce the effectiveness of active acoustic sensors [49,50] and can increase background reverberation, through scattering and absorption, of active acoustic transmission and reception. For instance, increased volume scattering from microbubbles and particles are documented

as limiting the smallest detectable target and accuracy of target tracking when using 200 and 420 kHz sidelooking echosounders in two Alaskan rivers [51]. Microbubbles are also a part of volume scattering in a volume of ensonified water with ACs [52] as they are with sonars. In fact, microbubbles' strong resonance at the frequencies of most ACs (1–3 MHz) makes them candidates for flow field measurements such as those of [52], who explored AC data at 3 MHz for bubble image velocimetry methods. Our research did not quantify the suspended microbubbles and thus the attenuation affects, though likely, are not known.

Of the 16 fish translocated to above the ARIS FOV, two were observed and two were possible detections. It is not known whether the remaining fish were not detected because they immediately swam outside of the FOV of the ARIS, or because the ARIS was not able to detect them. Ultimately, catches of longnose suckers and lake chubs were too low to make conclusions about the efficacy of using the ARIS for understanding the detection, classification, and behavior of small fish upstream of a turbine.

The angle of the ARIS relative to the water surface also affected image quality and, in turn, target detection. In the June 14 data, the ARIS was 0.75 m deep and the FOV was horizontal with no downward tilt. In this orientation, the top of the beams contacted the water surface, which included entrained air associated with the barge pontoons and instrument mounts. This unwanted backscatter was mostly located in range category "1" (Figure 6). The low ARIS CPUE value for this day may be attributed to the lower signal-to-noise ratio due to interference from the water surface and entrained air. In fact, June 14 is the only day that fewer targets were detected in range category "1" than in range category "0". Aiming adjustments on subsequent days improved the FOV by having the top of the beams pass underneath the water's surface without making contact and returning unwanted backscatter.

Using active acoustics to detect, classify, and numerate fish is an established technique and many applications have a lengthy history to document and mitigate challenges and limitations. Using the ARIS at Test Site 2 was challenging but the data were able to provide the information needed to apportion targets as likely or unlikely to interact with a CEC, which is the minimum information needed when monitoring for collision risk to fishes posed by CECs.

4.3. Recommendations and Future Research

While studies detailing successful applications of ACs are important references for determining appropriate methods from their use, studies where ACs failed to provide expected results are also critical [5]. Monitoring for the environmental effects of marine energy is a relatively new application of ACs. Methods for making informed decisions about collision risk using ACs and experimental methods are not yet well established and monitoring campaigns around each new CEC device and at each new test site encounter novel challenges. However, each one shines new light on the overall challenge of collision risk and brings the industry, researchers, and other stakeholders closer to the development of effective repeatable methods that can be transferred to future projects. These successes and challenges will inform collision risk for marine energy and allow for effective decision making by regulators. In the following sections, the challenges encountered in this study are used to inform recommendations for effective use of ACs and future research.

4.3.1. Fish Strike Observation

While relatively few field data collections have observed fish interactions with CECs to date, completed studies indicate that the determination of a blade strike or near-miss event is challenging with both VCs [10] and ACs [12]. Most studies to date observed few or no interactions between fish and CECS. While this is a positive outcome for informing collision risk, it does not provide new data to improve methods of observation. The research presented in this paper demonstrates successful observation of blade strike with artificial targets by an ARIS 3000 Explorer AC. While this single instance that used tethered artificial targets may not represent reality, it indicates that detection of a collision event with a

high-resolution AC is possible. Further scenarios with real or artificial targets, including targets with onboard sensors, [53,54] at various current speeds and using various turbine sizes will continue to fill data gaps and provide future users with the ability to make informed decisions. The ability to observe blade strike or near-field behavior with ACs may be scenario specific, but in turbid water ACs are the only sensor that may be able to perform this task.

4.3.2. Acoustic Camera Selection

Choosing an AC to inform collision risk for fishes and CECs begins with knowledge of the size of fishes expected at a specific site, along with an estimate of the distance from the AC installation that they are expected to be. Next, a researcher must determine if the fish size and detection range requirements are achievable with currently available technology. Knowledge of pixel size relative to fish size at expected ranges of detection will inform the number of pixels a fish is made up of in an image [55]. A single pixel may be enough for detection of a target but not enough for classification characteristics such as shape and movement. There is no fixed value of pixel size or ratio of fish length to pixel size. As a rule of thumb, a large fish target at close range is the best sampling scenario that provides the highest detection capabilities and target classification potential. As fish get smaller and farther from the AC, there will be a decrease in detection probability and classification accuracy [35,56].

Target detection and classification are also affected by the speed of the targets. Because all CEC technology depends on water currents, this challenge is a potential at all sites. For the ARIS, each frame is a mosaic of duty-cycled sets of equally spaced beams and frame rates are limited by the image frame production time. Fewer frames of an individual target reduce the total review time, making it more difficult to detect and classify targets. The ARIS used in this research can reduce the number of beams used to create an image frame in half the time by capturing data in 64 beams instead of all 128. The tradeoff is that cross-range pixel resolution doubles in size. For large targets consisting of many pixels this tradeoff may prove useful in having more frames with the target present and potentially providing enough information for review, such as movement, to classify it accurately. When researchers are choosing an AC, it is important that they consider the current velocity, expected target size, and image production time.

Attenuation of sound transmission and signal returns can limit the usefulness of ACs and was likely in the research presented here. The presence of unquantified, organic matter in the water at Test Site 2 likely had attenuation effects on the ARIS. Attenuation of active acoustics from various suspended matter such as sediment is documented but the authors know of no study that has addressed the attenuation from the matter observed at Test Site 2. Future research applications of active acoustics at Test Site 2 and other locations with similar river characteristics should attempt to quantify the volume of this organic matter as well as the volume reverberation and subsequent attenuation it will have on ACs. Researchers must be aware of organic matter such as this at data collection sites and prepare to overcome this with careful sensor selection. For instance, decreasing the operational frequency of the AC can reduce the attenuation effects of water column matter [49], but the tradeoff will usually be a reduction in the resolution of sample pixels that can negatively affect target detection and classification.

4.3.3. Informing AC Targets with Catch Data

In this study, physical capture was conducted with the IPT to correlate known fish species and lengths with targets observed in the ARIS. The IPT CPUE was low during data collection leaving few fish to compare with ARIS targets. Future research at Test Site 2 (or similar site) using ACs for target detection and catch data to infer target classification is recommended in the absence of interactions with turbines. Removing the turbine interaction component will allow data collection focused on correlating observed AC targets with fish catches and may provide target signatures to inform classification [57]. Studies

should be timed with fish migrations to maximize catch rates. Additionally, different types of fishing gear should be investigated to provide the highest efficiency.

Informing AC targets with catch data in the absence of turbine deployments should not take priority over taking advantage of CEC testing that occurs at Test Sites 1 and 2. CEC technology developers are continually creating and refining devices and the necessary iterative testing cycle to improve them will present opportunities to further monitor, test, and improve methods for observing fish interacting with CECs. We recommend that researchers work with test site operators and seek funding to support monitoring. A continually growing record of empirical data of fish interactions with CECs will improve the sensors and methods to effectively monitor and inform collision risk decision making overall.

4.3.4. Modeling

To date, several model types (e.g., encounter rate models [ERMs] and collision risk models [CRMs]) to inform collision risk of fishes with CECs have been introduced in the literature. Field observation data to parameterize ERMs and CRMs are rare [58] and the research presented in this paper exemplifies the difficulty faced at energetic sites where CECs are deployed. The acquisition of field data as fish are approaching a CEC often involves the use of active acoustics sensors [12] and the data provide density, abundance, or biomass estimates and may provide avoidance behavior information—all of which are useful inputs for ERMs and CRMs. Evasion behavior, strike, or near-miss information is also important empirical input for CRMs, allowing an accurate estimate of fishes that are likely to collide with the turbine and thus estimate possible injury or mortality.

Providing valid data for collision risk models will require refining the methods of data collection at CEC deployment locations. The solution will not be a one-size-fits-all prospect but will require detailed adjustments based on site characteristics. Locations with clear water and adequate light, such as Test Site 1, can likely be monitored with VCs that will provide intuitive, easy-to-interpret data streams. Other locations with turbid water that may include various forms of debris, such as Test Site 2, will require ACs. With continued iterative testing of data collection methods such as those presented in this paper, meaningful, repeatable data will result, allowing for the validation of models to inform collision risk decision making.

5. Conclusions

Marine energy is a nascent industry that is continuously changing as information is gathered and iterative testing cycles are conducted. This paper is part of a Special Issue that, in addition to addressing collision risk, investigates sensors and methods for the stressors, electromagnetic fields, underwater noise, changes in habitat, and anthropogenic light. The environmental monitoring that parallels technology development such as CEC testing is also changing, and therefore there are few established methods. The collision risk stressor is no exception and, to date, ACs have been one of the main sensors chosen to observe fish interactions with CECs especially in turbid water. As CEC testing continues, it will be important for researchers to take advantage of past applications of ACs and leverage the successes and methods used for collecting data, processing data, and presenting results for decision making that informs the determination of or reduces collision risk of fish with CECs. However, limitations and shortfalls are part of the research process that rarely see publication, are often vaguely reported, and are maintained as individual knowledge bases. Sharing information about these limitations and shortfalls is crucial to the development of improved and standardized data collection strategies.

This paper provides evidence that blade strike can be observed with an AC in a particular scenario. Further situations should be tested to accumulate a knowledge base of blade strike detection limitations and effective scenarios. Additionally, at Test Site 2 a high-resolution ARIS AC was used at close range to an installed CEC turbine to detect small, fast-moving targets in a turbid river with significant debris loads. The results provided

target detection with range information informing whether the target was moving in the path of the installed turbine or likely to pass on either side. However, classifying targets as fish or debris was challenging and further work will be required to determine if this is a solvable problem using the current technology capabilities of ACs.

These challenges to data collection are often part of the expert knowledge of users of ACs but are rarely addressed in peer-reviewed literature. Highlighting these challenges here will allow current and future users of ACs to have important information ahead of planning field campaigns and will also provide a foundation for asking questions and reaching out to subject matter experts that may be part of their institutions or found elsewhere in the research community. The application of ACs to inform determinations of collision risk is new and each data collection event will likely require some component of research in the absence of established methods. Continued expertise from the modeling community will also be needed as researchers work to refine data collection methods, thereby assuring that meaningful empirical inputs can be used to parameterize and refine collision risk models. We encourage researchers to document research aspects of their collision risk monitoring efforts, whether challenging or successful, and publish or share them in conference venues or webinar forums. There are a lot of lessons to be learned about using ACs to inform the determination of the risk of fish colliding with CECs.

The risk of fish colliding with CECs (i.e., turbines) is an environmental effects concern, and sensor installation and operation for monitoring is difficult due to the energetic environments and often turbid or dark water. Resolving blade strike or near-miss of a fish or target during monitoring is challenging, as is classifying targets as fish, debris, or other material. Determination of appropriate sensors for data collection campaigns is important to gain information on strike events and detect and classify fish. Two federally funded test site locations enabled AC data to be collected, thereby providing information about artificial, natural, and control-released fish targets near operational CEC turbines. Data collected at the first site allowed us to confirm artificial target strike with an AC by combining concurrent VC data. Data collection at the second site was challenging given the fast currents, turbid, debris-laden water, dynamic sensor mounting platform, and small fish targets, which provided scenarios to push the limits of the ARIS 3000 used. Both sites provided information to determine strengths, limitations, and future research paths for how best to monitor for the risk of fish collision with CEC turbines.

References

1.   Kilcher, L.; Fogarty, M.; Lawson, M. *Marine Energy in the United States: An Overview of Opportunities*; NREL/TP-5700-78773; National Renewable Energy Laboratory (NREL): Golden, CO, USA, 2021.

2.   Geerlofs, S. Marine energy and the new blue economy. In *Preparing a Workforce for the New Blue Economy*; Hotaling, L., Spinrad, R.W., Eds.; Elsevier: Cambridge, UK, 2021; pp. 171–178. [CrossRef]

3.   Kirke, B. Hydrokinetic turbines for moderate sized rivers. *Energy Sustain. Dev.* **2020**, *58*, 182–195. [CrossRef] [PubMed]

4.   Sparling, C.E.; Seitz, A.C.; Masden, E.; Smith, K. *2020 State of the Science Report, Chapter 3: Collision Risk for Animals around Turbines*; Pacific Northwest National Laboratory: Richland, WA, USA, 2020; pp. 29–65.

5.   Hasselman, D.J.; Barclay, D.R.; Cavagnaro, R.; Chandler, C.; Cotter, E.; Gillespie, D.M.; Hastie, G.D.; Horne, J.K.; Joslin, J.; Long, C. *2020 State of the Science Report, Chapter 10: Environmental Monitoring Technologies and Techniques for Detecting Interactions of Marine Animals with Turbines*; Pacific Northwest National Laboratory: Richland, WA, USA, 2020; pp. 176–213.

6.   Barr, Z.; Roberts, J.; Peplinski, W.; West, A.; Kramer, S.; Jones, C. The Permitting, Licensing and Environmental Compliance Process: Lessons and Experiences within US Marine Renewable Energy. *Energies* **2021**, *14*, 5048. [CrossRef]

7.   Peplinski, W.J.; Roberts, J.; Klise, G.; Kramer, S.; Barr, Z.; West, A.; Jones, C. Marine energy environmental permitting and compliance costs. *Energies* **2021**, *14*, 4719. [CrossRef]

8.   Hammar, L.; Andersson, S.; Eggertsen, L.; Haglund, J.; Gullström, M.; Ehnberg, J.; Molander, S. Hydrokinetic turbine effects on fish swimming behaviour. *PLoS ONE* **2013**, *8*, e84141. [CrossRef]

9.   Broadhurst, M.; Barr, S.; Orme, C.D.L. In-situ ecological interactions with a deployed tidal energy device; an observational pilot study. *Ocean Coastal Man.* **2014**, *99*, 31–38. [CrossRef]

10. Matzner, S.; Trostle, C.K.; Staines, G.J.; Hull, R.E.; Avila, A.; Harker-Klimes, G.E. *Triton: Igiugig Video Analysis-Project Report*; PNNL-26576; Pacific Northwest National Laboratory: Richland, WA, USA, 2017.

11. Nemeth, M.; Priest, J.; Patterson, H. *Assessment of Fish and Wildlife Presence Near Two River Instream Energy Conversion Devices in The Kvichak River, Alaska in 2014*; LGL Inc.: Sidney, BC, Canada, 2014.

12. Viehman, H.A.; Zydlewski, G.B. Fish interactions with a commercial-scale tidal energy device in the natural environment. *Estuaries Coasts* **2015**, *38*, 241–252. [CrossRef]

13. Bevelhimer, M.; Scherelis, C.; Colby, J.; Adonizio, M.A. Hydroacoustic assessment of behavioral responses by fish passing near an operating tidal turbine in the east river, New York. *Trans. Am. Fish. Soc.* **2017**, *146*, 1028–1042. [CrossRef]

14. Williamson, B.J.; Blondel, P.; Williamson, L.D.; Scott, B.E. Application of a multibeam echosounder to document changes in animal movement and behaviour around a tidal turbine structure. *ICES J. Mar. Sci.* **2021**, *78*, 1253–1266. [CrossRef]

15. Belcher, E.; Hanot, W.; Burch, J. Dual-frequency identification sonar (DIDSON). In Proceedings of the 2002 Interntional Symposium on Underwater Technology (Cat. No. 02EX556), Tokyo, Japan, 16–19 April 2002; pp. 187–192.

16. Bilgili, A.; Proehl, J.A.; Lynch, D.R.; Smith, K.W.; Swift, M.R. Estuary/ocean exchange and tidal mixing in a Gulf of Maine Estuary: A Lagrangian modeling study. *Estuar. Coast. Shelf Sci.* **2005**, *65*, 607–624. [CrossRef]

17. Kammerer, C. *Tidal Currents in the Piscataqua River, NH: 2007 National Current Observation Program Survey*; New Hampshire DES: Durham, NH, USA, 2007.

18. Wosnik, M.; Chancey, K.; Gagnon, I.; Baldwin, K.; Bell, E. The 'living bridge' project: Tidal energy conversion at an estuarine bridge-Deployment and First Data. In Proceedings of the 6th Marine Energy Technology Symposium (METS), Washington, DC, USA, 30 April–2 May 2018.

19. Chancey, K. *Assessment of the Localized Flow and Tidal Energy Conversion System at an Estuarine Bridge*; University of New Hampshire: Durham, NH, USA, 2019.

20. Wosnik, M.; O'Byrne, P.; Chancey, K.; Gagnon, I.; Bell, E. A cost-effective grid-connected scaled tidal energy test site at Memorial Bridge in Portsmouth, New Hampshire, USA. In Proceedings of the International Conference on Ocean Energy, Virtual, 28–30 April 2021.

21. Jump, S.; Courtney, M.B.; Seitz, A.C. Vertical distribution of juvenile salmon in a large turbid river. *J. Fish. Wildl. Manag.* **2019**, *10*, 575–581. [CrossRef]

22.   Johnson, J.; Toniolo, H.; Seitz, A.; Schmid, J.; Duvoy, P. *Characterization of the Tanana River at Nenana, Alaska, to Determine the Important Factors Affecting Site Selection, Deployment, and Operation of Hydrokinetic Devices to Generate Power*; Alaska Center for Energy and Power, Alaska Hydrokinetic Energy Research Center: Fairbanks, AK, USA, 2013; p. 130.

23.   Brabets, T.P.; Wang, B.; Meade, R.H. *Environmental and Hydrologic Overview of the Yukon River Basin, Alaska and Canada*; 99-4204; United States Geological Survey: Anchorage, AK, USA, 2000.

24.   Johnson, J.; Kasper, J.; Schmid, J.; Duvoy, P.; Kulchitsky, A.; Mueller-Stoffels, M.; Konefal, N.; Seitz, A. *Surface Debris Characterization and Mitigation Strategies and Their Impact on the Operation of River Energy Conversion Devices on the Tanana River at Nenana, Alaska*; Alaska Center for Energy and Power, Alaska Hydrokinetic Energy Research Center: Fairbanks, AK, USA, 2015.

25.   Seitz, A.C.; Moerlein, K.; Evans, M.D.; Rosenberger, A.E. Ecology of fishes in a high-latitude, turbid river with implications for the impacts of hydrokinetic devices. *Rev. Fish Biol. Fish.* **2011**, *21*, 481–496. [CrossRef]

26.   Bradley, P.T.; Evans, M.D.; Seitz, A.C. Characterizing the juvenile fish community in turbid Alaskan rivers to assess potential interactions with hydrokinetic devices. *Trans. Am. Fish. Soc.* **2015**, *144*, 1058–1069. [CrossRef]

27.   Todd, G.L. A lightweight, inclined-plane trap for sampling salmon smolts in rivers. *Alaska Fish. Res. Bull.* **1994**, *1*, 168–175.

28.   EPRI. *Assessment of Technologies to Study Downstream Migrating American Eel Approach and Behavior at Iroquois Dam and Beauharnois Power Canal*; 3002009406; Electric Power Research Institute: Palo Alto, CA, USA, 2017; p. 156.

29.   Viehman, H.A.; Zydlewski, G.B.; McCleave, J.D.; Staines, G.J. Using hydroacoustics to understand fish presence and vertical distribution in a tidally dynamic region targeted for energy extraction. *Estuaries Coasts* **2015**, *38*, 215–226. [CrossRef]

30.   Amaral, S.V.; Bevelhimer, M.S.; Čada, G.F.; Giza, D.J.; Jacobson, P.T.; McMahon, B.J.; Pracheil, B.M. Evaluation of behavior and survival of fish exposed to an axial-flow hydrokinetic turbine. *N. Am. J. Fish. Manag.* **2015**, *35*, 97–113. [CrossRef]

31.   Castro-Santos, T.; Haro, A. Survival and behavioral effects of exposure to a hydrokinetic turbine on juvenile Atlantic salmon and adult American shad. *Estuaries Coasts* **2015**, *38*, 203–214. [CrossRef]

32.   Cook, D.; Middlemiss, K.; Jaksons, P.; Davison, W.; Jerrett, A. Validation of fish length estimations from a high frequency multi-beam sonar (ARIS) and its utilisation as a field-based measurement technique. *Fish. Res.* **2019**, *218*, 59–68. [CrossRef]

33.   Kimball, M.E.; Rozas, L.P.; Boswell, K.M.; Cowan, J.H., Jr. Evaluating the effect of slot size and environmental variables on the passage of estuarine nekton through a water control structure. *J. Exp. Mar. Biol. Ecol.* **2010**, *395*, 181–190. [CrossRef]

34.   Able, K.W.; Grothues, T.M.; Rackovan, J.L.; Buderman, F.E. Application of Mobile Dual-frequency Identification Sonar (DIDSON) to Fish in Estuarine Habitats. *Northeast. Nat.* **2014**, *21*, 192–209. [CrossRef]

35.   Burwen, D.L.; Fleischman, S.J.; Miller, J.D. Accuracy and precision of salmon length estimates taken from DIDSON sonar images. *Trans. Am. Fish. Soc.* **2010**, *139*, 1306–1314. [CrossRef]

36.   Mueller, A.-M.; Burwen, D.L.; Boswell, K.M.; Mulligan, T. Tail-beat patterns in dual-frequency identification sonar echograms and their potential use for species identification and bioenergetics studies. *Trans. Am. Fish. Soc.* **2010**, *139*, 900–910. [CrossRef]

37.   Helminen, J.; O'Sullivan, A.M.; Linnansaari, T. Measuring Tailbeat Frequencies of Three Fish Species from Adaptive Resolution Imaging Sonar Data. *Trans. Am. Fish. Soc.* **2021**, *150*, 627–636. [CrossRef]

38.   Martignac, F.; Daroux, A.; Bagliniere, J.L.; Ombredane, D.; Guillard, J. The use of acoustic cameras in shallow waters: New hydroacoustic tools for monitoring migratory fish population. A review of DIDSON technology. *Fish Fish.* **2015**, *16*, 486–510. [CrossRef]

39.   Arnold, G. Movements of fish in relation to water. In *Animal Migration*; Aidley, D.J., Ed.; Cambridge University Press: New York, NY, USA, 1981; Volume 13, p. 55.

40.   Simmonds, E.J. *Fisheries Acoustics: Theory and Practice*; John Wiley & Sons: Hoboken, NJ, USA, 2008.

41.   Holmes, J.A.; Cronkite, G.M.; Enzenhofer, H.J.; Mulligan, T.J. Accuracy and precision of fish-count data from a "dual-frequency identification sonar" (DIDSON) imaging system. *ICES J. Mar. Sci.* **2006**, *63*, 543–555. [CrossRef]

42.   Mueller, A.-M.; Mulligan, T.; Withler, P.K. Classifying sonar images: Can a computer-driven process identify eels? *N. Am. J. Fish. Manag.* **2008**, *28*, 1876–1886. [CrossRef]

43.   Balk, H.; Lindem, T.; Kubecka, J. New Cubic Cross filter detector for multi beam data recorded with DIDSON acoustic camera. In Proceedings of the 3rd International Conference & Exhibition Underwater Acoustic Measurements: Technologies & Results, Peloponnese, Greece, 21–26 June 2009.

44.   Petreman, I.C.; Jones, N.E.; Milne, S.W. Observer bias and subsampling efficiencies for estimating the number of migrating fish in rivers using Dual-frequency IDentification SONar (DIDSON). *Fish. Res.* **2014**, *155*, 160–167. [CrossRef]

45.   Pham, A.H.; Lundgren, B.; Stage, B.; Jensen, J.A. Ultrasound backscatter from free-swimming fish at 1 MHz for fish identification. In Proceedings of the 2012 IEEE International Ultrasonics Symposium, Dresden, Germany, 7–10 October 2012; pp. 1477–1480.

46.   Staines, G.; Zydlewski, G.B.; Viehman, H.A.; Kocik, R. Applying Two Active Acoustic Technologies to Document Presence of Large Marine Animal Targets at a Marine Renewable Energy Site. *J. Mar. Sci. Eng.* **2020**, *8*, 704. [CrossRef]

47.   Medwin, H.; Clay, C.S. *Fundamentals of Acoustical Oceanography*; Academic Press: Cambridge, MA, USA, 1998. [CrossRef]

48.   Maxwell, S.L.; Gove, N.E. Assessing a dual-frequency identification sonars' fish-counting accuracy, precision, and turbid river range capability. *J. Acoust. Soc. Am.* **2007**, *122*, 3364–3377. [CrossRef]

49.   Richards, S.; Leighton, T. High frequency sonar performance predictions for littoral operations—the effects of suspended sediments and microbubbles. *J. Def. Sci.* **2003**, *8*, 1–7.

50. Richards, S.; White, P.; Leighton, T. Volume absorption and volume reverberation due to microbubbles and suspended particles in a ray-based sonar performance model. In Proceedings of the Seventh European Conference on Underwater Acoustics, Delft, The Netherlands, 5–8 July 2004; pp. 173–178.

51. Dahl, P.H.; Geiger, H.J.; Hart, D.A.; Dawson, J.J.; Johnston, S.V. *The Environmental Acoustics of Two Alaskan Rivers and Its Relation to Salmon Counting Sonars*; University of Washington: Seattle, WA, USA, 2001; p. 40.

52. Young, D.L.; McFall, B.C.; Bryant, D.B. Bubble image velocimetry with a field-deployable acoustic camera. *Meas. Sci. Technol.* **2018**, *29*, 125302. [CrossRef]

53. Martinez, J.J.; Deng, Z.; Titzler, P.S.; Duncan, J.P.; Lu, J.; Mueller, R.P.; Tian, C.; Trumbo, B.A.; Ahmann, M.L.; Renholds, J.F. Hydraulic and biological characterization of a large Kaplan turbine. *Renew. Energy* **2019**, *131*, 240–249. [CrossRef]

54. Deng, Z.; Duncan, J.; Arnold, J.; Fu, T.; Martinez, J.; Lu, J.; Titzler, P.; Zhou, D.; Mueller, R. Evaluation of boundary dam spillway using an autonomous sensor fish device. *J. Hydro-Environ. Res.* **2017**, *14*, 85–92. [CrossRef]

55. Zang, X.; Yin, T.; Hou, Z.; Mueller, R.P.; Deng, Z.D.; Jacobson, P.T. Deep learning for automated detection and identification of migrating American eel Anguilla rostrata from imaging sonar data. *Remote Sens.* **2021**, *13*, 2671. [CrossRef]

56. Cotter, E.; Polagye, B. Detection and classification capabilities of two multibeam sonars. *Limnol. Oceanogr. Methods* **2020**, *18*, 673–680. [CrossRef]

57. Francisco, F.; Sundberg, J. Detection of visual signatures of marine mammals and fish within marine renewable energy farms using multibeam imaging sonar. *J. Mar. Sci. Eng.* **2019**, *7*, 22. [CrossRef]

58. Buenau, K.E.; Garavelli, L.; Hemery, L.G.; García Medina, G. A Review of Modeling Approaches for Understanding and Monitoring the Environmental Effects of Marine Renewable Energy. *J. Mar. Sci. Eng.* **2022**, *10*, 94. [CrossRef]